

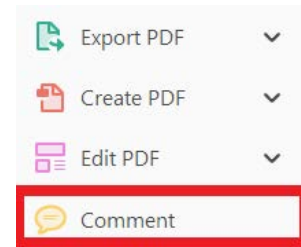
USING e-ANNOTATION TOOLS FOR ELECTRONIC PROOF CORRECTION

Required software to e-annotate PDFs: Adobe Acrobat Professional or Adobe Reader (version 11 or above). (Note that this document uses screenshots from Adobe Reader DC.)


The latest version of Acrobat Reader can be downloaded for free at: <http://get.adobe.com/reader/>

Once you have Acrobat Reader open on your computer, click on the [Comment](#) tab (right-hand panel or under the Tools menu).


This will open up a ribbon panel at the top of the document. Using a tool will place a comment in the right-hand panel. The tools you will use for annotating your proof are shown below:

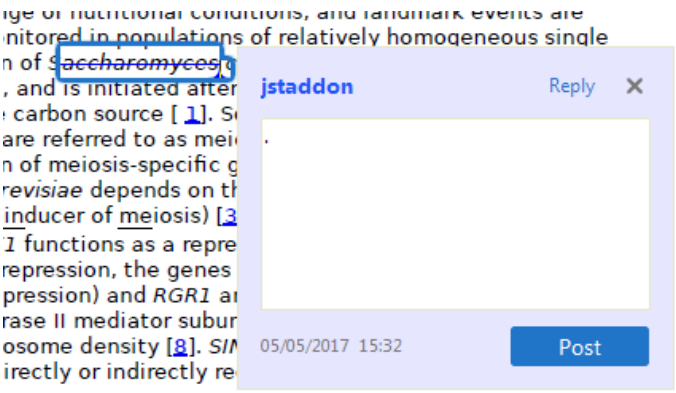


**1. Replace (Ins) Tool – for replacing text.**


 Strikes a line through text and opens up a text box where replacement text can be entered.

**How to use it:**

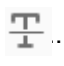
- Highlight a word or sentence.
- Click on .
- Type the replacement text into the blue box that appears.



**2. Strikethrough (Del) Tool – for deleting text.**

 Strikes a red line through text that is to be deleted.



**How to use it:**

- Highlight a word or sentence.
- Click on .
- The text will be struck out in red.



experimental data if available. For ORFs to be had to meet all of the following criteria:

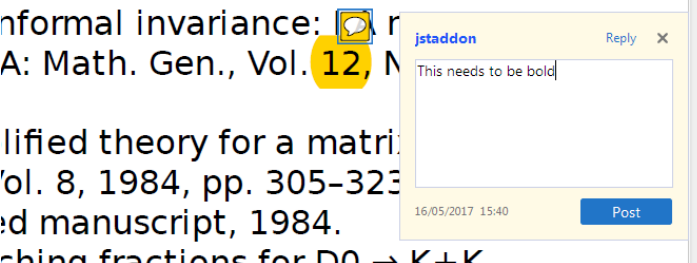
1. Small size (35-250 amino acids).
2. Absence of similarity to known proteins.
3. Absence of functional data which could not be the real overlapping gene.
4. Greater than 25% overlap at the N-terminal terminus with another coding feature; over both ends; or ORF containing a tRNA.

**3. Commenting Tool – for highlighting a section to be changed to bold or italic or for general comments.**

  Use these 2 tools to highlight the text where a comment is then made.


**How to use it:**

- Click on .
- Click and drag over the text you need to highlight for the comment you will add.
- Click on .
- Click close to the text you just highlighted.
- Type any instructions regarding the text to be altered into the box that appears.




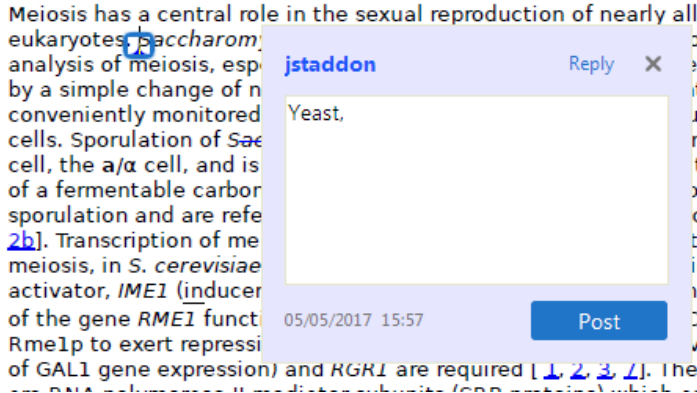
informal invariance: A: Math. Gen., Vol. 12, N  
 lified theory for a matrix  
 'ol. 8, 1984, pp. 305-323  
 ed manuscript, 1984.  
 ching fractions for  $D_0 \rightarrow K+K$   
 olation in  $D_0$  decays' Phys

**4. Insert Tool – for inserting missing text at specific points in the text.**

 Marks an insertion point in the text and opens up a text box where comments can be entered.


**How to use it:**

- Click on .
- Click at the point in the proof where the comment should be inserted.
- Type the comment into the box that appears.




Meiosis has a central role in the sexual reproduction of nearly all eukaryotes. *Saccharom* analysis of meiosis, esp by a simple change of n conveniently monitored cells. Sporulation of *Sae* cell, the a/ $\alpha$  cell, and is of a fermentable carbon sporulation and are refe [2b](#)]. Transcription of meiosis, in *S. cerevisiae* activator, *IME1* (inducer of the gene *RME1* funct Rme1p to exert repressi of GAL1 gene expression) and *RGR1* are required [1](#), [2](#), [3](#), [4](#)]. These ge or det e trigg its are us sin ne ty the a only d c gen tion o ional ne pro DNA-t ve ge

**5. Attach File Tool – for inserting large amounts of text or replacement figures.**

 Inserts an icon linking to the attached file in the appropriate place in the text.


**How to use it:**

- Click on .
- Click on the proof to where you'd like the attached file to be linked.
- Select the file to be attached from your computer or network.
- Select the colour and type of icon that will appear in the proof. Click OK.


The attachment appears in the right-hand panel.

chondrial preparator  
ative damage injury  
re extent of membra  
i, malondialdehyde (TBARS) formation.  
used by high perform

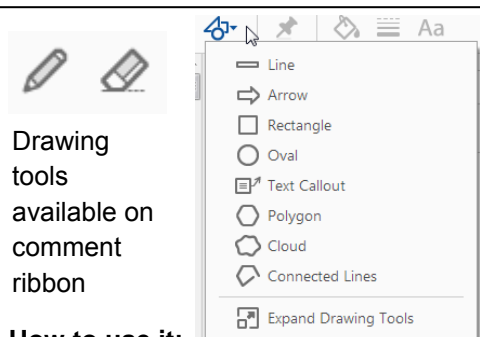
**6. Add stamp Tool – for approving a proof if no corrections are required.**

 Inserts a selected stamp onto an appropriate place in the proof.

**How to use it:**

- Click on .
- Select the stamp you want to use. (The **Approved** stamp is usually available directly in the menu that appears. Others are shown under *Dynamic*, *Sign Here*, *Standard Business*).
- Fill in any details and then click on the proof where you'd like the stamp to appear. (Where a proof is to be approved as it is, this would normally be on the first page).

of the business cycle, starting with the  
on perfect competition, constant ret  
production. In this environment goods  
extra costs should be set to zero for  
he market. The model is determined  
etermined by the model. The New-Key  
otaki (1987), has introduced produc  
general equilibrium models with nomin  
and real variables. Most of this literat

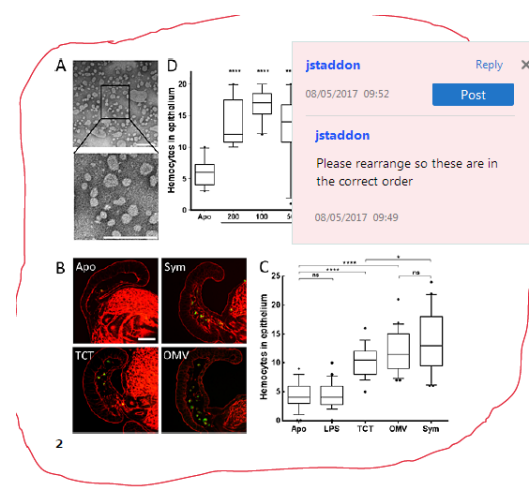


**How to use it:**

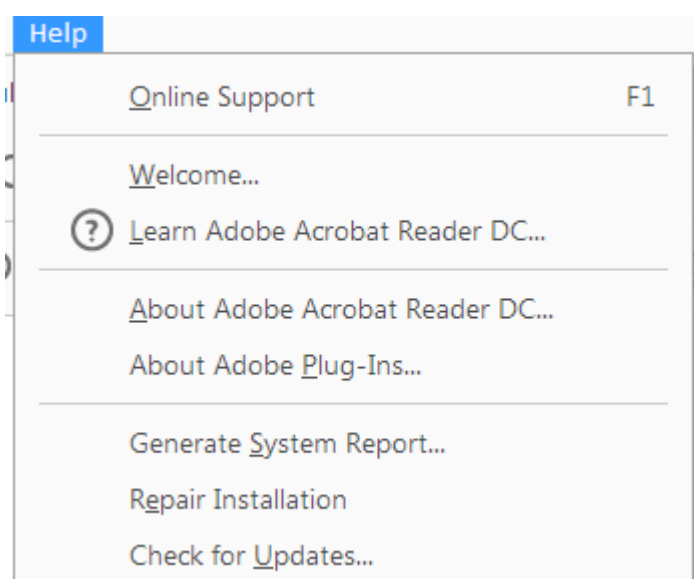
- Click on one of the shapes in the **Drawing Markups** section.
- Click on the proof at the relevant point and draw the selected shape with the cursor.
- To add a comment to the drawn shape, right-click on shape and select *Open Pop-up Note*.
- Type any text in the red box that appears.

**7. Drawing Markups Tools – for drawing shapes, lines, and freeform annotations on proofs and commenting on these marks.**

Allows shapes, lines, and freeform annotations to be drawn on proofs and for comments to be made on these marks.



For further information on how to annotate proofs, click on the **Help** menu to reveal a list of further options:



## Author Query Form

**Journal: The Structural Design of Tall and Special Buildings**

**Article: tal\_1586**

Dear Author,

During the copyediting of your paper, the following queries arose. Please respond to these by annotating your proofs with the necessary changes/additions.

- If you intend to annotate your proof electronically, please refer to the E-annotation guidelines.
- If you intend to annotate your proof by means of hard-copy mark-up, please use the standard proofing marks. If manually writing corrections on your proof and returning it by fax, do not write too close to the edge of the paper. Please remember that illegible mark-ups may delay publication.

Whether you opt for hard-copy or electronic annotation of your proofs, we recommend that you provide additional clarification of answers to queries by entering your answers on the query sheet, in addition to the text mark-up.

Query No.	Query	Remark
Q1	AUTHOR: As per journal style, author biography is required. Please provide.	
Q2	AUTHOR: Please confirm that forenames/given names (blue) and surnames/family names (vermilion) have been identified correctly.	
Q3	AUTHOR: Please verify that the linked ORCID identifiers are correct for each author.	
Q4	AUTHOR: As per journal style, author biography is required. Please provide.	
Q5	AUTHOR: Please check that authors' affiliations are correct.	
Q6	AUTHOR: Organization division or department name is required for Affiliation 3. Please provide.	
Q7	AUTHOR: Please check and confirm if the hierarchy of section headings are presented correctly.	
Q8	AUTHOR: Please define "SDOF" if this is an abbreviation or an acronym.	
Q9	AUTHOR: Please define "PEER NGA" if this is an abbreviation or an acronym.	
Q10	AUTHOR: In Table 1, please provide the full definition of "rec."	
Q11	AUTHOR: Please define "RC" if this is an abbreviation or an acronym.	

# The conditional mean spectra by disaggregating the eta spectral shape indicator

Mohammad Ali Mohandesi<sup>1</sup> | Alireza Azarbakht<sup>2</sup>  | Mohsen Ghafory-Ashtiany<sup>3</sup>

<sup>1</sup>Department of Civil Engineering, Science and Research Branch, Islamic Azad University, Tehran, Iran

<sup>2</sup>Department of Civil Engineering, Faculty of Engineering, Arak University, Arak, Iran

<sup>3</sup>International Institute of Earthquake Engineering and Seismology (IIEES), Tehran, Iran

## Correspondence

Alireza Azarbakht, Department of Civil Engineering, Faculty of Engineering, Arak University, Arak, Iran, PO Box 38156-88359. Email: a-azarbakht@araku.ac.ir

## Summary

Conditional spectra are a recent development in this field, which utilizes the advantages of spectral shape indicators, for example, epsilon and eta. The application of an eta indicator in conditional spectra calculations depends mainly on calculating the peak ground velocity epsilon, data about which are not readily available in the current literature. This issue has been solved by linear regression between the conventional epsilon and the peak ground velocity epsilon. However, not enough attention has been paid in the literature to the disaggregation of the eta indicator. For this reason, the disaggregation of seismic hazard based on the use of an eta indicator has been investigated in this paper, based on a simplified linear seismic source. The obtained results were compared with the available approach in the literature, which shows that this refinement has a meaningful effect on the conditional spectra specifically in the short period range. Furthermore, eta-based conditional spectra are used at different hazard levels to select ground-motion records. A three-storeyed building is then analysed, and the corresponding annual probability of failure is calculated based on the full dataset as well as on the records, which were selected based on conditional spectra.

## KEYWORDS

epsilon, eta, genetic algorithm, ground-motion prediction equation (GMPE), seismic hazard analysis

## 1 | INTRODUCTION

The selection of appropriate ground motion is a crucial element when assessing the seismic resistance of structures. Several methodologies have emerged, which are intended for use in the selection and scaling of ground-motion records (GMRs), for response history analyses<sup>[1-4]</sup>; other methods have also been proposed to further reduce the number of required ground motions while maintaining certain level of accuracy by using numerical techniques such as genetic algorithm.<sup>[5,6]</sup> The uniform hazard spectrum (UHS) is one of these developments that have been widely used in performance-based earthquake engineering. However, the implementation of UHS is somewhat conservative when it is used as a proxy for the ground-motion selection process. The reason is that it is challenging to find a record that has a spectrum as high as the UHS.<sup>[7]</sup> Furthermore, using the UHS may have a significant effect on fragility curves.<sup>[8]</sup>

Spectral shape indicators, for example, epsilon<sup>[9]</sup> and eta,<sup>[10]</sup> have been recently proposed. Conditional mean spectra have been obtained by employing the prementioned indicators, and they can be used as target design spectra, for example, conditional mean spectrum (CMS)<sup>[11]</sup> and eta-based conditional mean spectrum (ECMS).<sup>[12]</sup> Another approach is that of the generalized conditional intensity measure (GCIM), which has been proposed for the selection of ground motions for any form of seismic response analysis.<sup>[13-16]</sup> It has been shown that the estimation of seismic demand based on exact conditional spectra is unbiased in most considered cases. However, evaluations by the GCIM can be even more accurate, because they were unbiased for most—although not all—of the examined cases where estimates from the exact conditional spectra are biased.<sup>[17]</sup>

The idea of this paper comes from the fact that the eta indicator employs a conventional spectral acceleration epsilon ( $\epsilon_{S_a}$ ) in combination with the peak ground velocity (PGV) epsilon ( $\epsilon_{PGV}$ ). As the  $\epsilon_{PGV}$  is not common in seismic hazard disaggregation, a simple correlation formula was proposed and used in another study<sup>[10]</sup> to approximately assess the target  $\epsilon_{PGV}$  based on the conventional  $\epsilon_{S_a}$ . However, the validity of this simple formula needs to be further investigated, which is the primary focus of this paper. For this purpose, a case of the seismic hazard disaggregation of eta has been illustrated in this paper, to obtain the  $\epsilon_{PGV}$  explicitly. An ideal site with a single linear fault was assumed. The results show that the exact  $\epsilon_{PGV}$  differs to a certain extent from the results based on the available simple formula in the literature and that the resulting conditional spectra are sensitive to this refinement especially in the low period range.

## 2 | SPECTRAL SHAPE INDICATORS

Earthquake magnitude and distance parameters have been widely used to quantify earthquake events. The epsilon indicator, as defined in Equation (1), is also employed as a complementary parameter in such cases.

$$\epsilon = \frac{\ln S_a(T_1) - \ln \bar{S}_a(T_1)}{\sigma_{\ln S_a(T_1)}}, \quad (1)$$

where  $\ln S_a(T_1)$  is the (pseudo) spectral acceleration corresponding to the first period of a given structure and a specified damping ratio, that is,  $S_a(T_1, 5\%)$ , for a given record;  $\ln \bar{S}_a(T_1)$  and  $\sigma_{\ln S_a(T_1)}$  are the mean and standard deviations of the above-mentioned spectral acceleration obtained from a specific ground motion prediction equation (GMPE), respectively, for example,<sup>[18]</sup> CB08. Epsilon in Equation (1) should be calculated for an unscaled record and ideally has a zero mean and a standard deviation equal to unity. In other words, epsilon defines the number of standard deviations that a given record spectrum differs from the mean spectrum predicted by a specific GMPE.

The definition of epsilon is generalized, as written in Equation (2), in which it is based on an arbitrary.<sup>[10]</sup>

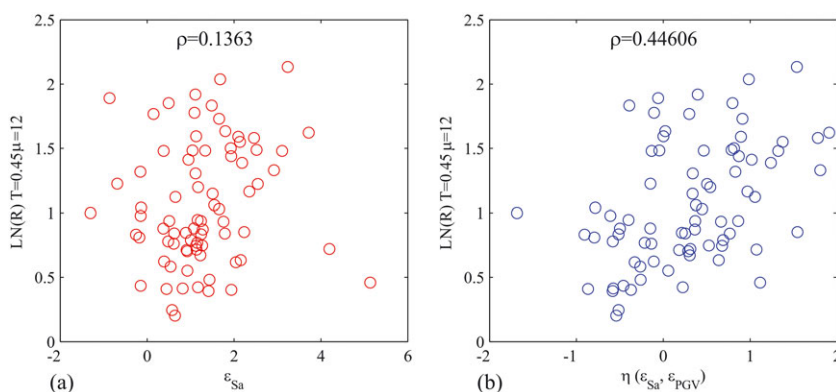
$$\epsilon_{IM} = \frac{\ln(IM) - \mu_{\ln(IM)}}{\sigma_{\ln(IM)}}, \quad (2)$$

where  $IM$  is an arbitrary IM for a given record;  $\sigma_{\ln IM}$  and  $\mu_{\ln IM}$  are the mean and standard deviation of the IM obtained from a specific GMPE, respectively, for example,<sup>[18]</sup> in this study.

The eta parameter was defined as a linear combination of the conventional  $\epsilon_{S_a}$  and the  $\epsilon_{PGV}$ . It has shown better performance when compared with the traditional<sup>[10]</sup>  $\epsilon_{S_a}$ . It was also demonstrated that eta has a higher correlation coefficient with the structural response when compared with the conventional<sup>[10]</sup>  $\epsilon_{S_a}$ . The original idea of introducing eta was aimed at combining the time domain IMs (i.e., the peak ground acceleration [PGA], the PGV, and the peak ground displacement) with the frequency domain IMs (i.e., the spectral acceleration). Several linear combinations were examined to find an appropriate formulation, and the best case was named eta as written in Equation (3), which had the highest correlation with the structural response.<sup>[10]</sup>

$$\eta = \epsilon_{S_a} - 0.823\epsilon_{PGV}. \quad (3)$$

Each epsilon as calculated by Equation (2) reflects some inherent information about the considered record. Thus combinations of a time domain IM with a frequency domain IM tend to increase eta efficiency. This efficiency is defined as the correlation between a given IM and the nonlinear structural response (here chosen as the collapse capacity). Figure 1 shows an example of an arbitrary single degree of freedom (SDOF) system considering eta and  $\epsilon_{S_a}$ . However, as a shortcoming, epsilon should be obtained for a specific hazard level. The standard probabilistic seismic hazard analysis (PSHA) usually, for a given magnitude and distance, provides particular ground-motion parameters besides epsilon and does not reflect any information about the PGV epsilon. Assuming equal values for these two epsilons seems inappropriate because similar



**FIGURE 1** The correlation between the nonlinear structural response (collapse capacity) of an arbitrary SDOF oscillator for (a)  $\epsilon_{S_a}$  and (b) eta index

amounts for the conventional spectral acceleration epsilon- and eta-based epsilon do not necessarily correspond to a specific hazard level. For this reason, the correlation between the traditional spectral acceleration epsilon and eta-based epsilon, at different periods, was studied, and a linear regression was obtained as written<sup>[10]</sup> in Equation (4). It is worth mentioning that the eta concept was derived based on a relatively large bin of earthquake events, which consists of 267 pairs of worldwide shallow crustal records with the magnitudes greater than 5.5 and distances<sup>[19]</sup> less than 100 km.

$$\varepsilon_{PGV} = C_1 \varepsilon_{S_a} + C_0. \quad (4)$$

As a direct approach to the record selection procedure, the eta-based epsilon is obtained based on Equation (4) for a specific hazard level. Equation (3) is then utilized to calculate the target eta. The records, which have the closest eta value to the target eta, are then chosen for further investigations in performance-based earthquake engineering. Another approach aims at calibrating Equation (3), to obtain a target eta, which would be identical to the target spectral acceleration epsilon. For this purpose, the coordinate transformation in Equation (3) was assumed as is shown in Equation (5).

$$\eta = k_0 + k_1(\varepsilon_{S_a} - 0.823\varepsilon_{PGV}). \quad (5)$$

By substituting Equation (4) into Equation (3) and equalizing the target eta with the target spectral acceleration epsilon, values for the constants  $k_0$  and  $k_1$  were obtained, as are shown<sup>[10]</sup> in Equation (6).

$$k_0 = \frac{bC_0}{1 - bC_1} = 0.485, \quad k_1 = \frac{1}{1 - bC_1} = 2.454. \quad (6)$$

By substituting these values into Equation (5), a new definition of eta was introduced, as is shown<sup>[10]</sup> in Equation (7).

$$\eta = 0.485 + 2.454\varepsilon_{S_a} - 2.020\varepsilon_{PGV}. \quad (7)$$

The target eta is now equal to the target spectral acceleration epsilon if Equation (7) is implemented.<sup>[10]</sup> In other words, and based on the eta concept, there are two possible approaches, which can be used when attempting to correctly select ground motion records (GMRs) for nonlinear dynamic analyses: (a) the target PGV epsilon is calculated based on Equation (4) versus the target epsilon, which is obtained based on the PSHA disaggregation analysis for a specific site. Equation (3) is then employed to get the target eta, which can be used to select records, that is, those records whose eta values—calculated for a specific record using Equation (3)—are closest to the target eta. (b) As a more straightforward approach, Equation (7) can be used to calculate each record's eta. Then those records, which have values of eta that are the closest to the target spectral acceleration epsilon (the target spectral acceleration epsilon is the same as in the previous approach), are selected.

This approach was verified by other researchers, for example, Eads et al. implemented epsilon, eta, and a new proposed spectral shape indicator and concluded that using eta produces a significantly stronger correlation with the logarithmic collapse intensities than when using a conventional epsilon, indicating that eta is indeed a better measure of spectral shape than epsilon.<sup>[20]</sup>

### 3 | DISAGGREGATION OF THE SEISMIC HAZARD

PSHA statistically combines all the possible earthquake events, which are likely to occur at a specific site. Additionally, it is possible to use a set of GMPEs, within the PSHA framework, to account for the epistemic uncertainty. The most convenient form of PSHA, for a single seismic source, is that shown<sup>[21]</sup> in Equation (8).

$$\lambda(y) = v \iint f_M(m) f_R(r) P[Y > y | m, r] dm dr, \quad (8)$$

where  $\lambda(y)$  is the rate of occurrence of earthquakes with an IM  $> y$ .  $f_M(m)$  and  $f_R(r)$  are the probability density functions associated with M and R, respectively.  $P[Y > y | m, r]$  is derived from an appropriate GMPE, and  $v$  is the rate of occurrence of earthquakes for a specific seismic source. Any additional seismic parameters, other than the magnitude and distance, can be accounted for within this integrant. For example, Equation (8) can be rewritten into Equation (9) by taking epsilon, as a function of the ground motion randomness, into consideration.

$$\lambda(y) = v \iiint f_M(m) f_R(r) f_\varepsilon(\varepsilon) P[Y > y | m, r, \varepsilon] dm dr d\varepsilon. \quad (9)$$

The most conventional IM is the (pseudo) spectral acceleration, which corresponds to the fundamental period of vibration of a given structure and a selected damping ratio, that is,  $S_a(T_1, 5\%)$ .  $S_a(T_1, 5\%)$  is used because the majority of hazard curves are available regarding spectral acceleration as a result of the PSHA values, which can be obtained from well-known ground-motion databases (e.g., those of the United States Geological Survey).

Disaggregation of seismic hazard, for a specific return period, was also introduced to obtain the contribution of the different seismic scenarios<sup>[21]</sup> within Equations 8–9. The disaggregation analysis is performable for an arbitrary set of seismic parameters, for example,  $M$ ,  $R$ , and  $\epsilon$ . The mathematical forms of the standard disaggregation for the parameters mentioned above are presented in Equations 10–12.

$$f_{M|S_0}(m) = \frac{\int \int f_M(m) f_R(r) f_\epsilon(\epsilon) P[Y > y | m, r, \epsilon] dr d\epsilon}{\lambda(y)}, \quad (10)$$

$$f_{R|S_0}(r) = \frac{\int \int f_M(m) f_R(r) f_\epsilon(\epsilon) P[Y > y | m, r, \epsilon] dm d\epsilon}{\lambda(y)}, \quad (11)$$

$$f_{\epsilon|S_0}(\epsilon) = \frac{\int \int f_M(m) f_R(r) f_\epsilon(\epsilon) P[Y > y | m, r, \epsilon] dm dr}{\lambda(y)}. \quad (12)$$

In this equation,  $f_{M|S_0}(m)$  is the contribution of the different magnitudes to the total hazard, and  $\lambda(y)$  is obtained from Equation (9). Equation (10) can be reorganized so that it can provide the disaggregation of distance, Equation (11), and different epsilon definitions, Equation (12). In this study, two different epsilon definitions were used, which are the conventional epsilon for spectral acceleration IM, as well as the epsilon for PGV. The disaggregation of the eta indicator is then calculated by combining the results of the two epsilons at the same hazard levels. The disaggregation epsilon bins were selected from  $-3$  to  $3$ , with an increment step of  $0.05$ .

## 4 | WHY DO WE NEED CONDITIONAL SPECTRA?

As suggested by most design regulations, the input for the estimation of the seismic response of structures consists of a set of GMRs in which the combined spectra of the records are compatible with a given design spectrum. It is clear that the most commonly used design spectrum is UHS. However, UHS ordinates in different period ranges are based on different event characteristics. In other words, UHS is not a good representation of a specific earthquake event because only rare events have spectra as high as UHS.<sup>[22,23]</sup> Thus, estimates of the seismic response of structures are frequently conservative when UHS is used as the target spectra.<sup>[22,23]</sup> To deal with this issue, new target spectra, referred to here as “conditional spectra,” were introduced to cope with the shortcomings of the UHS.<sup>[11]</sup> The advantages of spectral shape indicators can be used within this context to obtain more realistic spectra than the conventional UHS. The conditional spectra, based on spectral shape indicators, are briefly described in this section. A simple example is then provided to further clarify this issue.

### 4.1 | Conditional spectra based on the spectral acceleration epsilon indicator

The steps, which need to be performed in the calculation of conditional spectra, based on the spectral acceleration epsilon indicator, are summarized below<sup>[11]</sup>:

- Step 1. The target spectral acceleration epsilon, the target magnitude, and the target distance are obtained based on the seismic disaggregation analysis.<sup>[21]</sup> The seismic disaggregation analysis is performed for a specific point on the design spectra, which is usually at a period that is the same as the fundamental period of vibration of a given structure.
- Step 2. The mean and standard deviation for the spectral acceleration,  $\mu_{\ln S_0(M,R,T)}$  and  $\sigma_{\ln S_0(T)}$ , is obtained based on a specific GMPE. It should be mentioned that in this paper, the CB08 model is used.<sup>[18]</sup>
- Step 3. The spectral acceleration epsilon corresponding to periods other than the target period is obtained based on a correlation model, as is shown in Equation (13).

$$\mu_{\epsilon(T_i)|\epsilon(T^*)} = \rho(T_i, T^*) \epsilon(T^*), \quad (13)$$

where  $\mu_{\epsilon(T_i)|\epsilon(T^*)}$  is the mean conditional epsilon at the period  $T_i$ ,  $\rho(T_i, T^*)$  is the correlation between the epsilon values at the periods  $T_i$  and  $T^*$ , and  $\epsilon(T^*)$  is the target epsilon at the period  $T^*$ . A correlation model was proposed in another study,<sup>[9]</sup> as stated in Equation (14), which is valid for the period range of  $0.05$  to  $5$  s.

$$\rho(T_{\min}, T_{\max}) = 1 - \cos\left(\frac{\pi}{2} - \left(0.359 + 0.163 I_{(T_{\min} < 0.189)} \ln \frac{T_{\min}}{0.189}\right) \ln \frac{T_{\max}}{T_{\min}}\right), \quad (14)$$

where  $I_{(T_{\min} < 0.189)}$  is a function that is equal to unity in the case of  $T_{\min} < 0.189$ , otherwise it has a value of zero.  $T_{\min}$  and  $T_{\max}$  are the two assumed period values in which the correlation is investigated. More sophisticated correlation models have been proposed in other studies.<sup>[24,25]</sup>

Step 4. The CMS is obtained based on Equation (15).

$$\mu_{\ln S_a(T_i) | \ln S_a(T^*)} = \mu_{\ln S_a}(M, R, T_i) + \rho(T_i, T^*) \varepsilon(T^*) \sigma_{\ln S_a}(T_i), \quad (15)$$

where  $\mu_{\ln S_a}(M, R, T)$  and  $\sigma_{\ln S_a}(T)$  are calculated based on a GMPE model and the  $\rho(T_i, T^*)$  value is obtained either based on an available closed-form model or based on an analytical correlation from the ground-motion database. It should be emphasized that there are, in general, two available CMS, which are the approximate CMS<sup>[9]</sup> and the exact CMS.<sup>[26,27]</sup> The approximate CMS is based on the mean causal M, R, and the spectral acceleration epsilon, whereas the exact CMS combines all the M, R, and spectral acceleration epsilon cases from the disaggregation analysis.

## 4.2 | Conditional spectra based on an eta indicator

An eta indicator was proposed in a previous work.<sup>[10]</sup> It has a higher level of correlation with the nonlinear structural response when compared with the case of the conventional spectral acceleration epsilon. For this reason, it was used as a new proxy for the calculation of the conditional spectra.<sup>[12]</sup> The target spectral acceleration epsilon and the target eta are necessary to calculate the conditional spectra. However, the standard seismic disaggregation analysis only provides the target spectral acceleration epsilon, and no information about the target eta is available. On the other hand, in the study given in a previous study,<sup>[10]</sup> a linear-calibrated eta has used in which the target spectral acceleration epsilon was identical to the target eta. A CMS, with this assumption, was therefore proposed, as is shown in Equation (16).

$$S_a(T) = e^{\left( \mu_{\ln S_a} + \eta^{\text{target}} \sigma_{\ln S_a(T)} \left( \frac{\rho_{(\eta(T), \eta(T^*))} + 1.730}{2.730} \right) \right)}, \quad (16)$$

where  $\rho_{(\eta(T), \eta(T^*))}$  is the correlation coefficient between eta(T) and eta(T\*). Equation (16) can be rewritten as Equation (17), where  $\rho'_{(\eta(T), \eta(T^*))}$  is obtained based on Equation (18).

$$S_a(T) = \exp\left( \mu_{\ln S_a(T)} + \eta^* \sigma_{\ln S_a(T)} \rho'_{(\eta(T), \eta(T^*))} \right), \quad (17)$$

$$\rho'_{(\eta(T), \eta(T^*))} = \frac{\rho_{(\eta(T), \eta(T^*))} + 1.73}{2.730}, \quad (18)$$

A closed form model was proposed in a previous study<sup>[12]</sup> to obtain  $\rho'_{(\eta(T), \eta(T^*))}$ . The stepwise calculation of the conditional spectra, based on the exact eta, is as follows:

Step 1. Considering the seismic source and its characteristics and the structural properties like the first mode period ( $T^*$ ), PSHA can be performed, and the results can be obtained regarding  $S_a$  versus hazard and PGV versus hazard.

Step 2. By considering a hazard level and obtaining its equivalent  $S_a$ , it is possible to compute a related probability density function based on Equation (10) and the mean value of magnitude using Equation (19). The mean value of the distance can also be calculated using Equation (19).

$$\bar{M} = E(M | S_a > y) = \sum_j m_j P(M = m_j | S_a > y). \quad (19)$$

Step 3. By employing the same approach as Step 2 for a known PGV, it will be possible to compute the mean  $\bar{\varepsilon}_{PGV}$  using Equations 20–21:

$$f_{\varepsilon_{PGV} | S_a, y}(\varepsilon_{PGV}, y) = \frac{1}{\gamma(PGV > y)} \int \int f_{M, R, \varepsilon}(m, r, \varepsilon) P(PGV > y | m, r, \varepsilon) dr dm, \quad (20)$$

$$\bar{\varepsilon}_{PGV} = E(\varepsilon_{PGV} | PGV > y) = \sum_j \varepsilon_{PGVj} P(\varepsilon_{PGV} = \varepsilon_{PGVj} | PGV > y). \quad (21)$$

Step 4. Using Equation (3), it will be possible to calculate  $\eta(T^*)$  for any desired hazard value and obtain an  $\eta(T^*)$  versus hazard diagram.

Step 5. Having  $\bar{M}$ ,  $\bar{R}$  and employing GMPEs, it is possible to compute  $\sigma_{\ln S_a}(\bar{M}, \bar{R})$  and  $\mu_{\ln S_a(T)}(\bar{M}, \bar{R}, T)$  for a specific value of T.

Step 6. Computation of  $\rho(T_i, T^*)$ , which is the correlation between the  $\eta$  values at the periods  $T_i$  and  $T^*$ , that is, an ensemble of 267 ground-motion pairs, were selected and processed by using CB08 to obtain  $\eta$  for a period range between 0.01 and 5 with an increment of 0.01 s.

Step 7. Repeating the above steps to calculate the exact ECMS by using Equations 22a–22c.

$$(a) \mu_{\ln S_a(T)} = \bar{\mu}_{\ln S_a(T)} + \sigma_{\ln S_a} \varepsilon, \quad (b) \mu_{\ln S_a(T)} = \bar{\mu}_{\ln S_a(T)} + \sigma_{\ln S_a} \varepsilon, \quad (c) \mu_{\ln S_a(T) | \ln S_a(T^*)} = \mu_{\ln S_a(T)}(\bar{M}, \bar{R}, T) + \sigma_{\ln S_a}(\bar{M}, \bar{R}) \left[ \rho \eta(T^*) + 0.823 \varepsilon_{PGV} \right]. \quad (22)$$

The process of calculating the proposed ECMS for a specific hazard level and a given value for  $T^*$  is shown in Figure 2.

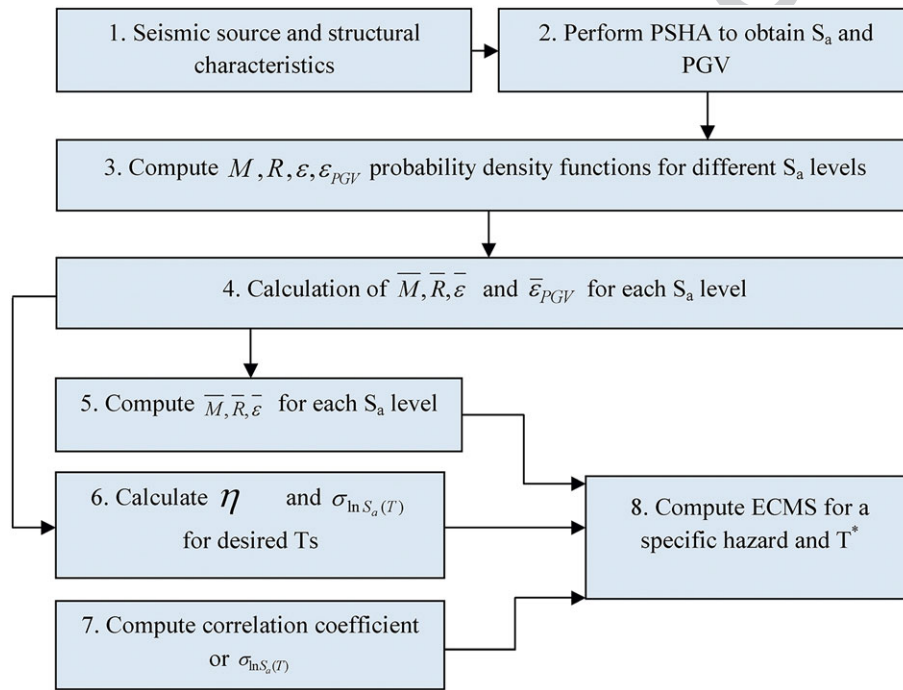


## 5 | THE CONDITIONAL SPECTRA FOR AN IDEAL SITE

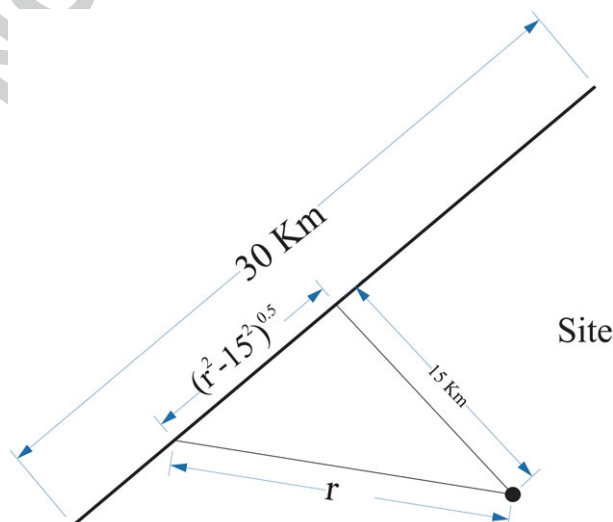
As mentioned in the previous section, the goal of this paper is to calculate the conditional spectra based on the refined eta approach. Therefore, an ideal site was assumed with a single line source as shown in Figure 3. The line source length is equal to 30 km, and the site is located 15 km (in the middle) from this source. The Gutenberg–Richter parameters were assumed as  $a = 1.29$  and  $b = 1.32$ . The other seismic parameters<sup>[18]</sup> were assumed as  $M_{\max} = 7$ ,  $M_0 = 5$ ,  $R_{jb} = 2$  km,  $\Delta = 90^\circ$ , and  $V_{s30} = 460$  m/s<sup>2</sup>.  $M_{\max}$  is the maximum earthquake the source can produce or upper magnitude limit,  $M_0$  is the minimum magnitude or lower magnitude limit,  $R_{jb}$  is the Joyner–Boore distance (km),  $\Delta$  is an average dip of the rupture plane (degree), and  $V_{s30}$  is shear wave velocity averaged over top 30 m (m/s).

By assuming a uniform distribution for the probability of exceedance, the cumulative distribution function for the distance parameter is written in Equation (23).

$$F_R(r) = \begin{cases} 0 & r < 15 \\ \frac{2\sqrt{r^2 - 15^2}}{30} & 15 \leq r < 21 \\ 1 & r > 21 \end{cases} \quad (23)$$



**FIGURE 2** The process of calculating the proposed eta-based conditional mean spectrum for a specific hazard and  $T^*$



**FIGURE 3** The ideal line source as the only causal event

The probability density function of the distance parameter is thus written in Equation (24).

$$f_R(r) = \frac{d}{dr}F_R(r) = \begin{cases} \frac{r}{15\sqrt{r^2 - 15^2}} & 15 \leq r < 21 \\ 0 & \text{otherwise} \end{cases} \quad (24)$$

The magnitude and distance models were used with an appropriate GMPE (CB08 in this study) to obtain the seismic hazard curves based on Equation (8). The results are shown in Figure 4 for the PGV and  $S_a$  ( $T = 1$  s, 5%).

It is worth mentioning that Equation (10) is used to obtain the magnitude distribution that causes  $S_a > y$ . This equation is adapted in the cases of distance and epsilon by using Equations 11–12. The mean values of  $M$ ,  $R$ , and epsilon, are then obtained, which are named the target magnitude, the target distance, and the target spectral acceleration epsilon, respectively. In other words, these target values are obtained for each point of the hazard curve. These target values are calculated for all of the hazard curve points in the case of magnitude, distance, PGV epsilon, and spectral acceleration epsilon, as are shown in Figure 5a–d.

The seismic hazard versus the eta indicator is obtained by combining Figures 5a,b. Note that this combination is performed based on Equation (3) for equal hazard values. The result is called the specific target eta and will be compared with different approximate eta values.

Two different approximate eta values are named: (a) a previous study<sup>[10]</sup> proposed that Equation (4) should be used in Equation (3). With this simplification, there is no need to have a target PGV epsilon, and (b) the relationship between the PGV epsilon and the spectral acceleration epsilon is computed for each period considered using disaggregation, and then linear regression is performed on these exact data to obtain a new approximation. As seen in Figure 6, a meaningful difference is observed between the approximation presented in the previous study<sup>[10]</sup> and the exact solution for a specific period. As seen in Figure 7, the calculations for other natural periods are repeated and compared with the approximate value suggested in the previous study.<sup>[10]</sup> The proposed relationship between  $\epsilon_{PGV}$  and  $\epsilon_{S_a}$  is given in Equation (25).

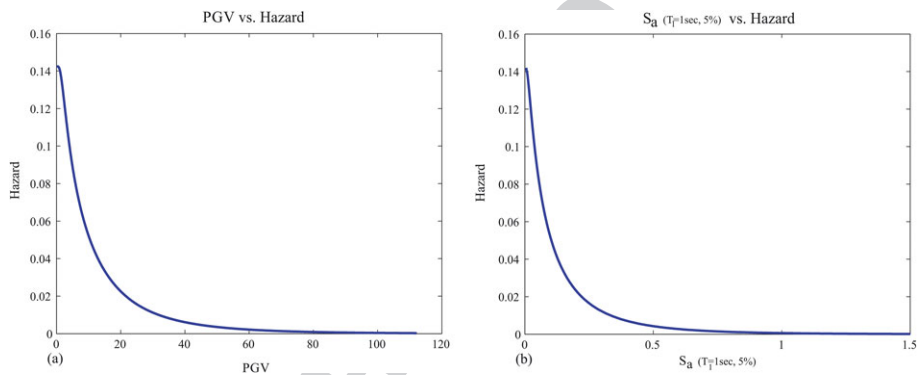


FIGURE 4 (a) Seismic hazard curve versus peak ground velocity; (b) seismic hazard curve versus  $S_a$  ( $T = 1$  s, 5%)

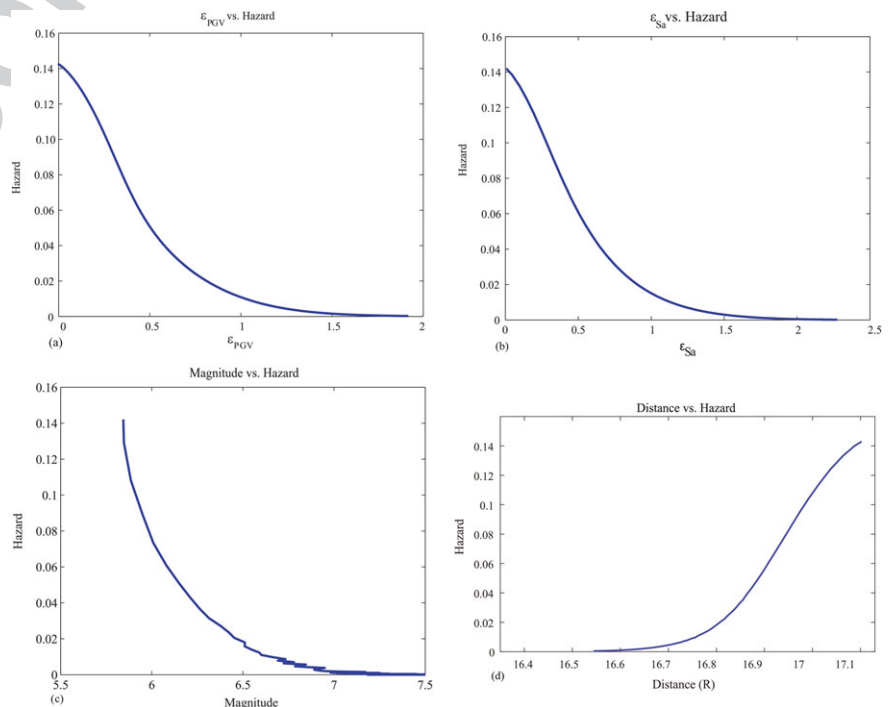


FIGURE 5 The mean values of (a)  $\epsilon_{PGV}$ , (b)  $\epsilon_{S_a}$ , (c) magnitude, and (d) distance (km) obtained from the disaggregation analysis

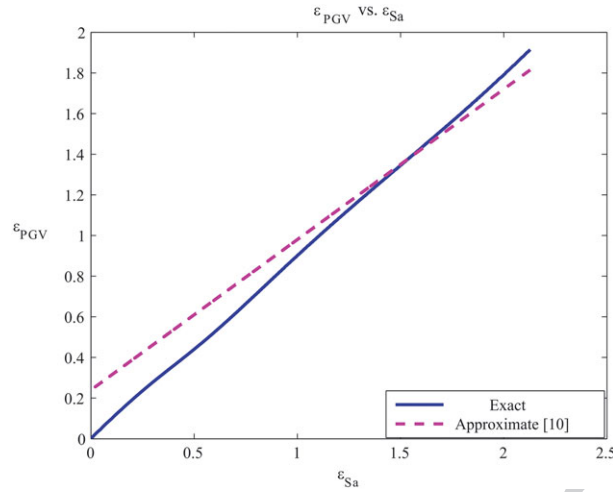


FIGURE 6 The exact and approximate relationship between  $\epsilon_{PGV}$  and  $\epsilon_{Sa}$  in the case of  $T = 1$  s

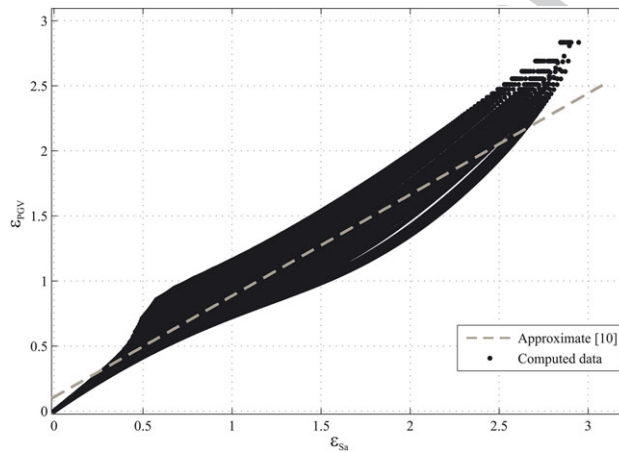


FIGURE 7 The exact and approximate relationship between  $\epsilon_{PGV}$  and  $\epsilon_{Sa}$  in the case of all the considered spectral accelerations

Figure 8 shows the hazard curve versus the eta parameter for three cases: the exact hazard curve based on Equation (3) and combining Figures 5a,b, the approximate hazard curve based on the proposal,<sup>[10]</sup> and the approximate hazard curve based on Equation (25). As can be seen in Figure 8, the approximate hazard curve based on the previous study<sup>[10]</sup> has meaningful differences with the exact solution especially in the low range of eta values. Additionally, the proposed relationship based on Equation (25) can be adequately matched with the exact answer.

F8

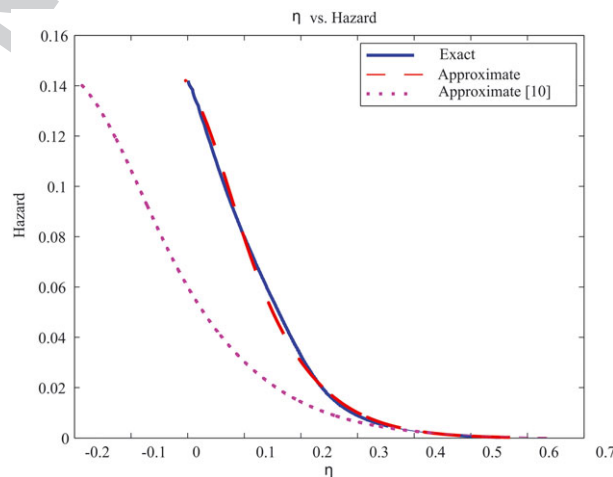


FIGURE 8 Eta versus hazard based on the exact and different approximate approaches.

However, there remains a concern, which has not yet been addressed. This is how much the conditional spectra are sensitive to this refinement. For this reason, the UHS, the ECMS based on the<sup>[10]</sup> approximation, and the ECMS based on the eta disaggregation for  $T^* = 1$  are shown in Figure 9. As can be seen from this figure, the difference between the two mentioned ECMS cases are apparent in the low range of **F9** periods, that is, 0.3 to 1 s. However, in the extended period range, all the conditional spectra are well matched.

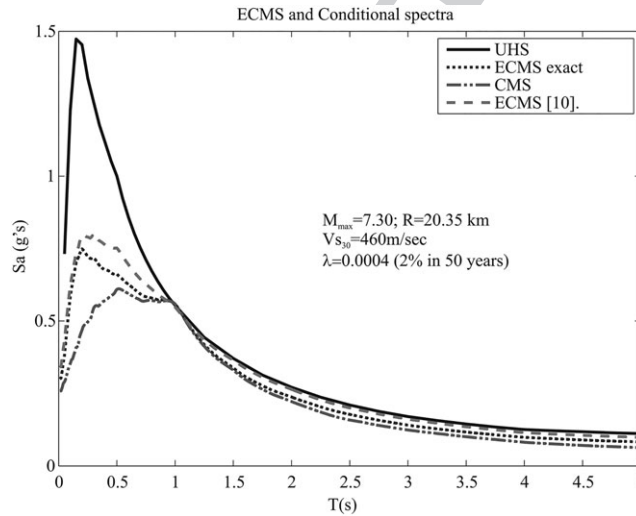
$$\varepsilon_{PGV} = 0.8509\varepsilon_{Sa} + 0.0495. \quad (25)$$

## 6 | APPLICATION OF THE PROPOSED REFINED ECMS IN GROUND-MOTION SELECTION

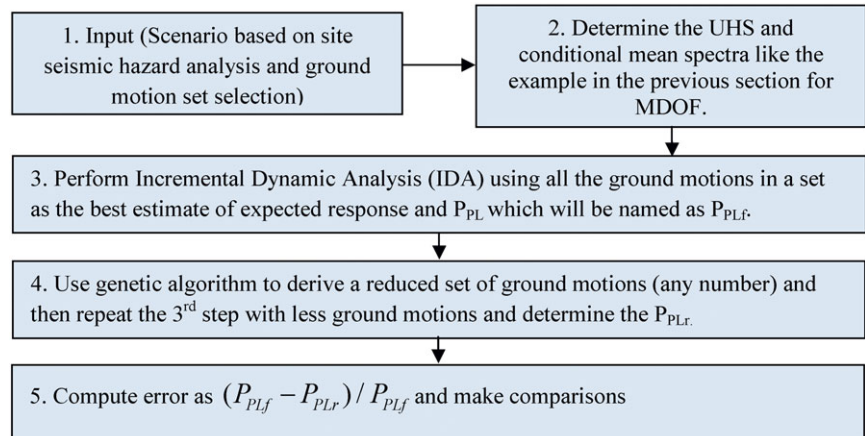
In this section, the results of the proposed refined ECMS are compared with the results of the CMS and ECMS based on the previous study.<sup>[10]</sup> The mean annual frequency (MAF) of failure, Equation (26), defined in another study,<sup>[28]</sup> was considered as a measure of accuracy, which is a kind of convolution of the fragility and hazard curve.

$$P_{PL} = \int_0^{\infty} p_{LS}(x) \cdot |d\lambda_{IM}(x)|, \quad (26)$$

where  $p_{LS}(x)$  is the fragility curve or the probability that a definite limit state is reached in a definite IM ( $IM = x$ ) and that  $|d\lambda_{IM}(x)|$  is the absolute derivative of hazard. A three-storey building, which will be defined later, with laboratory test results, was used for the analysis. First, the general definitions and assumptions are discussed, and then the numerical results are presented. Figure 10 shows the steps involved in the determination **F10** of  $P_{PL}$  for all ground motions by using incremental dynamic analysis (IDA)<sup>[29]</sup> and reduced set selected based on the conditional spectra for the three-storey multidegree of freedom system (MDOF). To further reduce the numerical effort and check the efficiency of the studied and proposed methods, a set of 20 ground motions out of a set of 44 were selected using the genetic algorithm, to obtain the parameters of the reduced number of ground motions, which are shown by the index "r." By defining the errors as  $(P_{PLf} - P_{PLr})/P_{PLf}$ , a negative error value implies overestimation of  $P_{PLf}$ . The results of all ground motions in a set are considered as the best estimate of the response.



**FIGURE 9** Uniform hazard spectrum, conditional mean spectrum, eta-based conditional mean spectrum (ECMS) based on<sup>[10]</sup> approximation, and ECMS based on exact  $\eta$  disaggregation



**FIGURE 10** Steps involved in the determination of  $P_{PL}$  using incremental dynamic analysis and conditional spectra

## 6.1 | Input data and general definitions

A hazard curve based on PSHA is considered to determine the  $P_{PL}$  for the the three-storey MDOF system. In this hazard curve,  $S_a(1\text{ s})$  for 50% in 50 years, 10% in 50 years, and 2% in 50 years are equal to (0.19, 0.4, 0.65)g, respectively. The site was located at a distance of 15 km from an active fault on very dense soil and soft rock ( $V_{s30} = 460\text{ m/s}$ , NEHRP Site Class C). It is usually beneficial to estimate the hazard especially in the region of interest by a power-law relationship<sup>[30]</sup>:  $H_{Sa} = k_0 (S_a)^k$ . In this case, the constant coefficients were defined as  $k_0 = 1 \times 10^{-4}$  and  $k = -3.4396$ . A damping ratio of 5% was assumed for all the analyses.

Furthermore, a confidence level (CL) is computed corresponding to an allowable probability noted<sup>[31]</sup> as  $P_0$ . In Equation (5),  $k_x$  is the standard Gaussian variate with the probability  $x$  of not being exceeded, and  $\beta_U$  is the dispersion measure representing the total epistemic uncertainty in the IM-based approach.

$$e^{k_x} \leq \frac{P_0}{P_{PL}} e^{-k\beta_U}. \quad (27)$$

$k_x$  and the corresponding CL is computed by solving Equation (27) and using the usual distribution table. In the calculation of fragility curves, to determine the probability and the MAF of collapse, a dispersion of 0.34 was taken into account and added to the randomness dispersion computed from the IDA analyses to account for the modelling uncertainty as suggested by Haselton.<sup>[32]</sup> The error definition for CL is the same as the error defined previously for  $P_{PL}$  computation.

A general far-field ground-motion set as suggested by FEMA,<sup>[33]</sup> consisting of 22 ground-motion pairs recorded at sites located more than 10 km from the fault rupture, was selected from another study<sup>[34]</sup> to calculate IDA curves needed for the  $P_{PL}$  estimation. Figure 11 shows the acceleration spectra of the ground-motion chosen records, their means, and their respective means  $\pm$  standard deviations. The SGMRs details are listed in Table 1.

## 6.2 | Three-storey RC structure

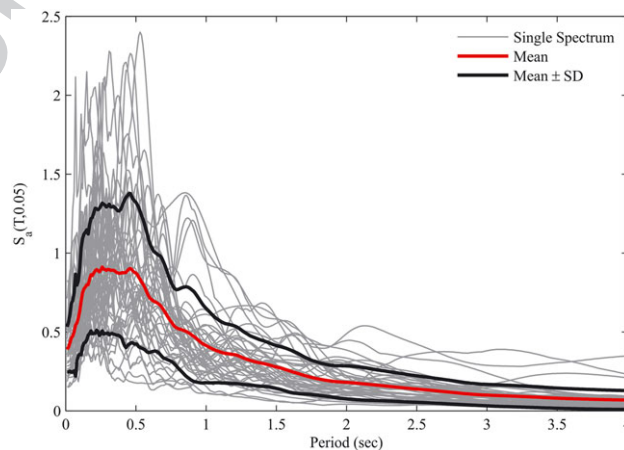
The three-storey 3D RC structure designed by another study<sup>[35]</sup> for which a pseudodynamic experiment was performed at full scale at the ELSA Laboratory, within the European research project SPEAR ("Seismic performance assessment and rehabilitation of existing buildings")<sup>[36]</sup> was selected. The first natural period ( $T_1$ ) is equal to 0.85 s, and the idealized period for the corresponding first mode equivalent SDOF system is 0.92 s (see Figure 12). A more detailed explanation of the model and a comparison of experimental and numerical results can be found in a previous research.<sup>[37]</sup> The nonlinear response history analyses (NLRHA) were performed for the weak (X) direction of the structure. Figure 12 shows the IDA curves, the pushover curve in the X direction, and the equivalent SDOF backbone behaviour. The force-displacement envelope of the SDOF model was obtained by dividing the forces and displacements of the idealized pushover curve by the transformation factor<sup>[38]</sup>  $\Gamma$ .

Theoretically, the introduced method can be used for any structure like bridges, dams, storage, and tanks. In the modelling of structures, advanced topics can also be considered, which has not been addressed in this research.<sup>[39-41]</sup>

To evaluate the annual probability of failure using the proposed method, it is first essential to compute the mean spectra using a different method discussed in this manuscript, that is, UHS, CMS, ECMS,<sup>[10]</sup> and the refined ECMS (see Figure 13).

## 6.3 | Performing the IDA

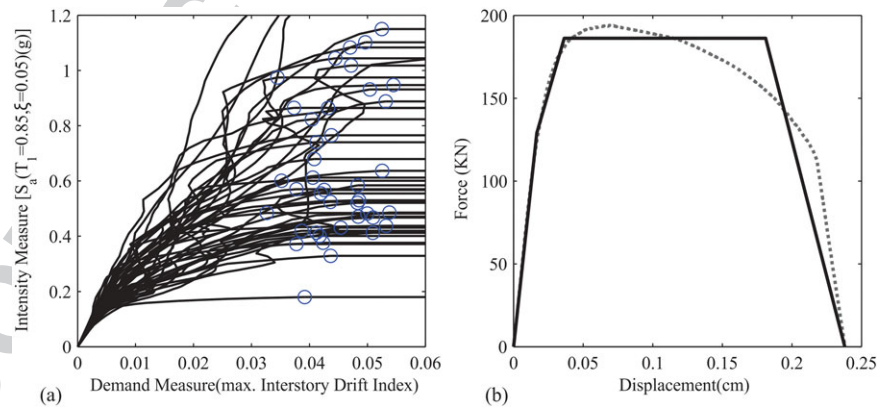
IDA is a powerful tool in performance-based engineering. Performing IDA is necessary to evaluate the seismic demand and capacity and their distributions.<sup>[42]</sup> The results can be used to calculate the fragility curve, which is needed in  $P_{PL}$  calculations. The obtained results for all the ground



**FIGURE 11** Acceleration spectra of the 22 selected ground-motion records, the mean, and the respective mean  $\pm$  standard deviation

**TABLE 1** ID numbers of the different employed SGMRs

ID	PEER NGA rec. #	Event, year	Mw	$R_{ave}$	ID	PEER-NGA rec. #	Event, year	Mw	$R_{ave}$	Q9	Q10
1	953	Northridge, 1994	6.7	13.3	23	848			19.85		
2	1602	Duzce, Turkey, 1999	7.1	12.2	24	960	Northridge, 1994	6.7	11.9		
3	1602			12.2	25	752	Loma Prieta, 1989	6.9	22.1		
4	1787	Hector Mine, 1999	7.1	11.2	26	752			22.1		
5	1787			11.2	27	767			12.5		
6	169	Imperial Valley, 1979	6.5	22.25	28	767			12.5		
7	169			22.25	29	1633	Manjil, Iran, 1990	7.4	12.8		
8	174			13	30	1633			12.8		
9	174			13	31	721	Superstition Hills, 1987	6.5	18.35		
10	953	Northridge, 1994	6.7	13.3	32	721			18.35		
11	1111	Kobe, Japan, 1995	6.9	16.15	33	725			11.45		
12	1111			16.15	34	725			11.45		
13	1116			23.8	35	829	Cape Mendocino, 1992	7	11.1		
14	1116			23.8	36	829			11.1		
15	960	Northridge, 1994	6.7	11.9	37	1244	Chi-Chi, Taiwan, 1999	7.6	12.75		
16	1158	Kocaeli, Turkey, 1999	7.5	14.5	38	1244			12.75		
17	1158			14.5	39	1485			26.4		
18	1148			12.05	40	1485			26.4		
19	1148			12.05	41	68	San Fernando, 1971	6.6	24.35		
20	900	Landers, 1992	7.3	23.7	42	68			24.35		
21	900			23.7	43	125	Friuli, Italy, 1976	6.5	15.4		
22	848			19.85	44	125			15.4		

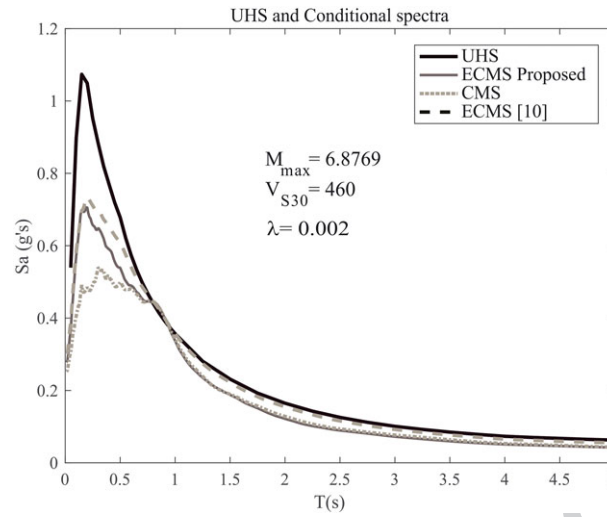
**FIGURE 12** (a) Incremental dynamic analysis curves; (b) pushover curve in the X direction and the equivalent idealized SDOF behaviour

motions in the far-field set are considered as the best estimate, then using genetic algorithm a reduced set of ground motions will be selected to compare the results and evaluate the efficiency of conditional spectra.

In order to use a genetic algorithm, a fitness function should be introduced. In this study, the area under mean acceleration response spectrum has been selected as fitness parameter such that the area under the mean spectrum of the reduced set, as closely as possible, matches the area under the spectrum of different methods for the obtaining of CMS, that is, CMS, ECMS,<sup>[10]</sup> and the refined ECMS. Thus, there will be three sets of reduced GMRs, each consisting of 20 ground motions (out of 44).

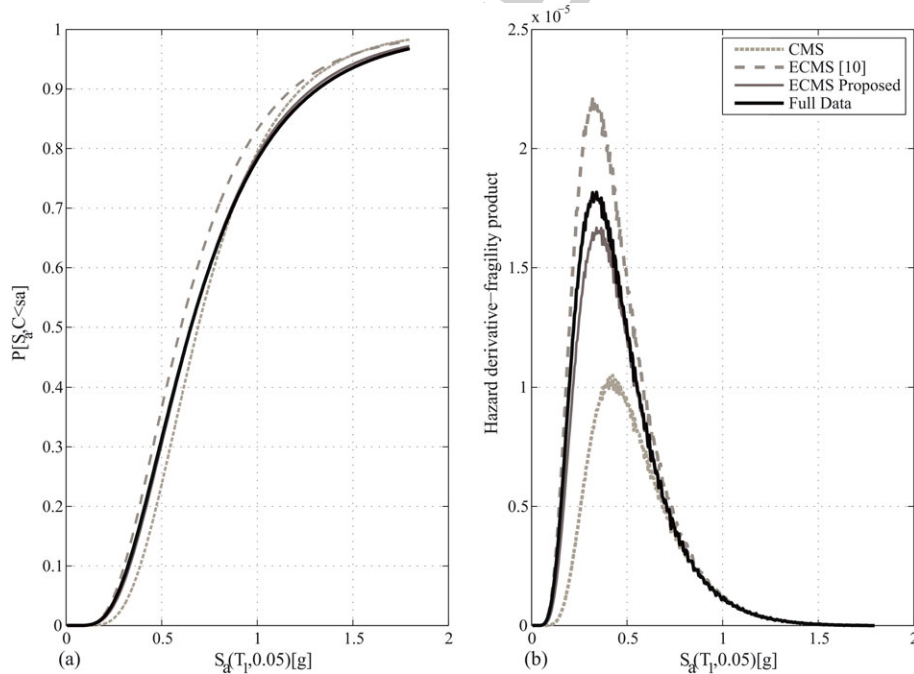
$$Error(s, N, T_0, T_1) = \frac{\int_{T_0}^{T_1} |\bar{S}_{a,N} - \bar{S}_{a,s}| dT}{A_{\bar{S}_{a,s}(T_0, T_1)}} \quad (28)$$

In Equation (28),  $s$  is the number of selected ground-motion subsets to estimate the mean spectrum, which has been selected as 20 in this research.  $N$  is the number of all ground motions considered for structural analysis and equals 44 here. The area under acceleration response spectrum for a reduced set of ground motions in the range of  $T_0$  and  $T_1$  has been denoted as  $A_{\bar{S}_{a,s}(T_0, T_1)}$ .  $\bar{S}_{a,N}$  is mean response spectrum considering all ground motions, and  $\bar{S}_{a,s}$  is for the reduced set of ground motions. The genetic algorithm examines different combinations of 20 ground motions out of 44 and sorts them so the best set can be used for the further process.



**FIGURE 13** Uniform hazard spectrum, conditional mean spectrum, eta-based conditional mean spectrum (ECMS)<sup>[10]</sup> and proposed ECMS for hazard level 10% in 50 years

Figure 14 (a) Shows the fragility curves and the hazard derivative–fragility product for the different methods in the case of 10% in 50 years hazard level. As can be seen from Tables 2–4, the  $P_{PL}$  and CL are computed and compared with the best estimate obtained from the full data set as well as the error attributed to each method.



**FIGURE 14** Fragility curve and hazard derivative–fragility product for different methods for 10% in 50 years hazard

**TABLE 2** Comparison of obtained results using full and reduced ground motions and different spectra 2% in 50 years

Method	$\beta_R$	$e^{H_{lnS_d}(T_1, col)}$	$P_{PL}$	Error in $P_{PL}$	CL% <sup>*</sup>	Error in CL%
Best estimate	0.43	0.6529	0.0016	—	17.2	—
CMS	0.4725	0.7042	0.0014	8.114	20.92	-21.6
ECMS Mousavi	0.4221	0.6792	0.0014	11.724	21.6	-25.5
ECMS proposed	0.4298	0.6797	0.0014	10.105	21.256	-23.5

Note. CL: confidence level; CMS: conditional mean spectrum; ECMS: eta-based conditional mean spectrum.

**TABLE 3** Comparison of obtained results using full and reduced ground motions and different spectra 10% in 50 years

Method	$\beta_R$	$e^{H_{lnS_0}(T_1, col)}$	$P_{PL}$	Error in $P_{PL}$	CL%*	Error in CL%
Best estimate	0.43	0.6529	0.0016	—	58	—
CMS	0.2961	0.6906	0.0010	38.7	69.7	-20.2
ECMS <sup>[10]</sup>	0.4065	0.6008	0.0019	-17.8	53.5	7.7
ECMS proposed	0.4039	0.6549	0.0015	7.02	59.96	-3.39

Note. CL: confidence level; CMS: conditional mean spectrum; ECMS: eta-based conditional mean spectrum.

**TABLE 4** Comparison of obtained results using full and reduced ground motions and different spectra 50% in 50 years

Method	$\beta_R$	$e^{H_{lnS_0}(T_1, col)}$	$P_{PL}$	Error in $P_{PL}$	CL%*	Error in CL%
Best estimate	0.43	0.6529	0.0016	—	90.07	—
CMS	0.4434	0.7014	0.0013	14.32	89.8	0.2919
ECMS Mousavi	0.3493	0.6686	0.0012	23.42	93.23	-3.505
ECMS proposed	0.4453	0.6635	0.0016	0.1361	89.095	1.082

Note. CL: confidence level; CMS: conditional mean spectrum; ECMS: eta-based conditional mean spectrum.

## 7 | CONCLUSIONS

The conditional spectrum based on the eta indicator was investigated in this paper. The results found on the two considered approaches are compared, which are (a) the conditional spectra based on the disaggregation of eta and (b) the conditional spectra based on the available approximation in the literature.

- The results show that the available approximation formula in the literature has a significant bias in the low period range. However, they are identical in the range of higher natural periods.
- A new approximation is proposed in this paper based on the eta disaggregation results to refine the approximation approach, which provided more appropriate structural performance evaluation regarding calculating MAF.
- The results of a three-storey building studied in this paper, considering three different hazard levels, indicate that using the proposed ECMS, it is possible to accurately predict the fragility curve and the product of the hazard derivative–fragility, which in turn will result in acceptable  $P_{PL}$  calculations with a reduced number of GMRs, in comparison with other methods studied in this article.
- The results of an eight-storey and a 12-storey RC frames, which have not been presented here for brevity, also show that the proposed ECMS in this article can accurately predict their performance in terms of calculations of the probability of failure in comparison with other methods studied here.

It is worth mentioning that the obtained results are case specific to the single site considered in this study. The results need to be regenerated for other site cases.

## ACKNOWLEDGEMENTS

To implement CB08 NGA GMPE in the current study, essential information about the NGA project, as well as ground-motion records bin and numerical programs, were used using the publicly available resource on the Pacific Earthquake Engineering Research Next Generation Attenuation Project web site at <http://peer.berkeley.edu/ngawest/index.html> (last accessed August 2013). The authors are very grateful to the two anonymous reviewers for their constructive and valuable comments.

## ORCID

Alireza Azarbakht  <https://orcid.org/0000-0003-3627-652X>

## REFERENCES

- [1] A. Catalan, A. Benavent-Climent, X. Cahis, *Soil Dyn. Earthq. Eng.* **2010**, 30(1–2), 40. <https://doi.org/10.1016/j.soildyn.2009.09.003>
- [2] E. I. Katsanos, A. G. Sextos, G. D. Manolis, *Soil Dyn. Earthq. Eng.* **2010**, 30(4), 157. <https://doi.org/10.1016/j.soildyn.2009.10.005>
- [3] C. B. Haselton, A. S. Whittaker, A. Hortacsu, J. W. Baker, J. Bray, D. N. Grant, Selecting and scaling earthquake ground motions for performing response-history analyses. 15WCEE 2012; Lisboa, Portugal.
- [4] Peer, GMSM, C. B. Haselton, Editor. Evaluation of ground motion selection and modification methods: predicting median interstorey drift response of buildings. PEER Report 2009/01, Pacific Engineering Research Center, University of California, Berkeley, California.
- [5] A. Azarbakht, M. Dolšek, *J. Struct. Eng. (ASCE)* **2011**, 137(3), 445. [https://doi.org/10.1061/\(ASCE\)ST.1943-541X.0000282](https://doi.org/10.1061/(ASCE)ST.1943-541X.0000282)
- [6] H. Kayhani, A. Azarbakht, M. Ghafory-Ashtiany, *Build* **2013**, 22, 1279. <https://doi.org/10.1002/tal.1006>



- [7] M.W. McCann, J.W. Baker, A. Gupta, Development of a seismic fragility methodology for nuclear power plant structures, CUREE-Kajima joint research program project report 2010; Richmond, Ca.
- [8] C. B. Haselton, J. W. Baker, Ground motion intensity measures for collapse capacity prediction, choice of optimal spectral period and effect of spectral shape, 8th National Conference on Earthquake Engineering 2006.
- [9] J. W. Baker, C. A. Cornell, *Earthq. Eng. Struct. Dyn.* **2006**, 35(9), 1077. <https://doi.org/10.1002/eqe.571>
- [10] M. Mousavi, M. Ghafory-Ashtiany, A. Azarbakht, *Earthq. Eng. Struct. Dyn.* **2011**, 40, 1403. <https://doi.org/10.1002/eqe.1096>
- [11] J. W. Baker, *ASCE J. Struct. Eng.* **2011**, 137(3), 322.
- [12] M. Mousavi, M. Shahri, A. Azarbakht, *Nucl. Eng. Des.* **2012**, 252, 27.
- [13] B. A. Bradley, *Earthq. Eng. Struct. Dyn.* **2010**, 39, 1321. <https://doi.org/10.1002/eqe.995>
- [14] B. A. Bradley, *Soil Dyn. Earthq. Eng.* **2012**, 40, 48. <https://doi.org/10.1016/j.soildyn.2012.04.007>
- [15] K. Tarbali, B. A. Bradley, Scenario-based ground-motion selection using the generalized conditional intensity measure (GCIM) approach, 10th U.S. National Conference on Earthquake Engineering, 2014, Anchorage, Alaska.
- [16] K. Tarbali, B. A. Bradley, *Earthq. Eng. Struct. Dyn.* **2015**, 44, 1601. <https://doi.org/10.1002/eqe.2546>
- [17] N. S. Kwong, A. K. Chopra, *Earthq. Eng. Struct. Dyn.* **2016**, 45, 757. <https://doi.org/10.1002/eqe.2683>
- [18] K. W. Campbell, Y. Bozorgnia, *Earthq. Spectra* **2008**, 24(1), 139. <https://doi.org/10.1193/1.2857546>
- [19] J. W. Baker, Vector-valued ground motion intensity measures for probabilistic seismic demand analysis, Report #150, John A.Blume Earthquake Engineering Center 2005, Stanford, CA. p. 321.
- [20] L. Eads, E. Miranda, D. Lignos, *Earthq. Eng. Struct. Dyn.* **2016**, 45(10), 1643. <https://doi.org/10.1002/eqe.2739>
- [21] R. McGuire, *Bull. Seismol. Soc. Am.* **1995**, 85(5), 1275.
- [22] J. W. Baker, C. A. Cornell, *Earthq. Eng. Struct. Dyn.* **2005**, 34(10), 1193. <https://doi.org/10.1002/eqe.474>
- [23] J. J. Bommer, S. G. Scott, S. K. Sarma, *Soil Dyn. Earthq. Eng.* **2000**, 19(4), 219. [https://doi.org/10.1016/S0267-7261\(00\)00012-9](https://doi.org/10.1016/S0267-7261(00)00012-9)
- [24] J. W. Baker, N. Jayaram, *Earthq. Spectra* **2008**, 24(1), 299.
- [25] A. Azarbakht, M. Shahri, M. Mousavi, *Bull Earthq Eng* **2014**, 13(3), 777. <https://doi.org/10.1007/s10518-014-9651-8>
- [26] H. Ebrahimian, A. Azarbakht, A. Tabandeh, A. A. Golafshani, *Soil Dyn. Earthq. Eng.* **2012**, 39, 61. <https://doi.org/10.1016/j.soildyn.2012.03.004>
- [27] T. Lin, S. C. Harmsen, J. W. Baker, N. Luco, *Bull. Seismol. Soc. Am.* **2013**, 103(2A), 1103. <https://doi.org/10.1785/0120110293>
- [28] B. Ellingwood, *Nucl. Eng. Des.* **1990**, 123(2), 189. [https://doi.org/10.1016/0029-5493\(90\)90237-R](https://doi.org/10.1016/0029-5493(90)90237-R)
- [29] D. Vamvatsikos, C. A. Cornell, *Earthq. Eng. Struct. Dyn.* **2002**, 31(3), 491. <https://doi.org/10.1002/eqe.141>
- [30] C. A. Cornell, F. Jalayer, R. O. Hamburger, D. A. Foutch, *J. Struct. Eng. (ASCE)* **2002**, 128(4), 526. <https://doi.org/10.1.1.476.7071>
- [31] F. Jalayer, C. A. Cornell, A technical framework for probability-based demand and capacity factor (DCFD) seismic formats 2003. Rep. No. RMS-43, RMS program, Stanford Univ., Stanford, Calif.
- [32] C. B. Haselton, G. G. Deierlein, Assessing Seismic collapse safety of modern reinforced concrete moment-frame buildings, PEER Report 2007/08, Pacific Engineering Research Centre, University of California, Berkeley, CA.
- [33] Federal Emergency Management Agency, Quantification of building seismic performance factors, FEMA P695, Prepared by Applied Technology Council for the Federal Emergency Management Agency 2009, Redwood City, CA
- [34] Pacific Earthquake Engineering Research Center, Strong motion database 2005, Available from: <http://peer.berkeley.edu/nga>, [last accessed: August 2013]
- [35] M. N. Fardis, Design of an irregular building for the SPEAR project-description of the three-storeyed structure 2002, University of Patras, Greece.
- [36] P. Negro, E. Mola, F. J. Molina, Magonette GE, Full-scale testing of a torsionally unbalanced three-storey nonseismic RC frame 2004. Proceedings of the 13th World Conference on Earthquake Engineering 2002, Vancouver, Canada; 968.
- [37] P. Fajfar, M. Dolšek, D. Marušič, A. Stratan, *Earthq. Eng. Struct. Dyn.* **2006**, 35(11), 1359. <https://doi.org/10.1002/eqe.583>
- [38] P. A. Fajfar, *Earthq. Spectra* **2000**, 16(3), 573. <https://doi.org/10.1193/1.1586128>
- [39] M. Mahdavi, M. R. Davoodi, A. Mostafavian, Determination of joint stiffness of a three story steel frame by finite element model updating, proceedings of the 15th world conference on earthquake Engineering, 2012.
- [40] N. Hosseinzadeh, H. Kazem, M. Ghahremannejad, N. Kazem, *J. Loss Prev. Process Ind.* **2013**, 26(4), 666. <https://doi.org/10.1016/j.jlp.2013.01.004>
- [41] M. Ghahremannejad, A. Abolmaali, *Eng. Struct.* **2018**, 169, 226. <https://doi.org/10.1016/j.engstruct.2018.05.048>
- [42] N. Su, X. Lu, Y. Zhou, T. Y. Yang, *Struct. Des. Tall Special Build.* **2017**, 26(8), 1356. <https://doi.org/10.1002/tal.1356>

#### AUTHOR BIOGRAPHIES

Mohammad Ali Mohandesi \*\*\*

Alireza Azarbakht \*\*\*

Mohsen Ghafory-Ashtiany \*\*\*

**How to cite this article:** Mohandesi MA, Azarbakht A, Ghafory-Ashtiany M. The conditional mean spectra by disaggregating the eta spectral shape indicator. *Struct Design Tall Spec Build.* 2018;e1586. <https://doi.org/10.1002/tal.1586>